ence on Robotics and Automat
St. Louis, Missouri, March 2
28, 1985.

ON THE OPTIMAL CONTROL OF ROBOTIC MANIPULATORS WITH ACTUATOR AND END-EFFECTOR CONSTRAINTS

Z. Shiller
Research Assistant

S. Dubowsky
Professor

Department of Mechanical Engineering
Massachusetts Institute of Technology
Cambridge, MA 02139

ABSTRACT

The motion of current industrial manipulators is typically controlled so that tasks are not done in a minimum time optimal manner. The result is substantially lower productivity than that potentially possible. Recently a computationally efficient algorithm has been developed to find the true minimum time optimal motion for a manipulator moving along a specified path in space that uses both the full nonlinear dynamic character of the manipulator and the constraints imposed by its actuators[1,2]. A Computer Aided Design (CAD) implementation of the algorithm called OPTARM is described which can treat practically general six degree-of-freedom manipulators. Examples are presented which show OPTARM to be a useful design tool for manipulators, their tasks and work places. The algorithm is extended in OPTARM to include the constraints imposed by manipulator payloads and end-effectors.

I. Introduction

The productivity of many industrial robotic manipulator tasks can be improved by having manipulators move more quickly. But several factors limit manipulator speeds, such as the finite capabilites of a system's actuators and the level of dynamic forces which the object being manipulated can tolerate without damage or being pulled out of the gripper. Even more important, the designs of current manipulator controllers do not permit industrial manipulators to move as quickly as they might, because they do not use effectively the full capabilities of their actuators, nor operate at or near the limits imposed by their payloads or end-effectors.

Manipulator dynamics are highly nonlinear and complex. Their actuators are required to produce complex, time varying torques or forces in order for the manipulator to follow even relatively simple paths; the dynamic forces at the payload are equally complex. Today's commercial manipulators are programmed to move along their paths with constant accelerations and velocities. The magnitudes of these velocities and accelerations are usually chosen by trial and error so that the actuators will not saturate at any point along the path. If the actuators attempt to exceed their saturation levels at any point the manipulator will leave its path. Such deviations are highly undesirable and potentially dangerous, particularly in highly structured industrial environments. Since the actuators may be near saturation at only a few points on the path, they will operate at less than their capacity at most points. Obviously a manipulator could operate faster by utilizing its full capacity at every point along the path.

The dynamic forces acting on the payload at high speed motion pose additional limits on performance, as they may be too high for some fragile or sensitive objects, or the dynamic load on the payload may be higher than the gripping forces which it holds. Gripping force can be limited by the gripper design, or by the structural strength of the object. Violating the end-effector gripping force or payload force limits are obviously equally undesirable.

This paper presents a Computer Aided Design (CAD) optimal control technique called OPTARM (Optimal Time Control of Articulated Robotic Manipulators) which insures that a manipulator operates to the full capacity of its actuators and achieves true minimum time motions.

The minimum time optimal control problem for manipulators is: given both the required initial and end states, and the dynamic properties and constraints on system motions, find the path and motion along it so that the final state is reached in minimum time. This general problem is difficult because while conventional optimal control theory is well developed for linear systems, it is difficult to apply to coupled nonlinear dynamic systems with complex constraints, such as robotic manipulators. It has been applied to very simplified models of the manipulators without path constraints[3-3,12]. These studies have shown that this type of approach is computationally very intensive. Moreover, path constraints (due to obstacles) are important factors in practical applications.

Other studies have considered the optimal time problem for manipulators as they move along specified paths chosen to avoid obstacles[7-11]. The problem here is to find the motion along the path as a function of time so that the task is completed in minimum time without exceeding the capabilities of the system. While this approach can easily consider limits on the system's motions, such as those imposed by obstacles, the

traveling time will be longer than permitting the system to find its own optimal path. None the less, these studies have not produced a true time optimal solution for this problem.

However, a recently developed algorithm for the minimum time control of manipulators moving along a prescribed path has proved to be rigorously optimal[1,2]. It uses the full nonlinear dynamics model. Actuators' constraints may be arbitrary functions of the system state. This algorithm also has been shown to be computationally efficient even for six degree-of-freedom manipulators since it does not require the usual extensive multiparameter iteration common in optimal control[3,4]. The OPTARM system is based on this algorithm with an extension to include payload and gripper dynamic constraints. OPTARM, with its interactive graphics capabilities, has proven to be a practical tool for designing general articulated robotic manipulators, their tasks, and work places. Examples are presented here for a 6 degree-of-freedom manipulator. The results show that task times are significantly reduced by the use of OPTARM. It has also been used as a key element in higher level optimal task planning[5].

II. The Time Optimal Control Algorithm

The basic time optimal control algorithm used here is derived in References [1] and [2]. The algorithm obtains the open loop torques/forces for the time optimal motion of a manipulator along a prescribed path, subject to actuator constraints. It also yields the optimal motion which can be used in closed loop control[6]. The method is applicable to manipulators with rigid links for which the dynamic model and the joint coordinates can be defined for any point on the path.

The approach uses a full nonlinear dynamic model of a manipulator which can be written as:

$$M\,\ddot{\underline{\theta}} + \dot{\underline{\theta}}^T C\,\dot{\underline{\theta}} + \underline{G} = \underline{T} \qquad (1)$$

where M is a 6x6 inertia matrix, C is a 6x6x6 coriolis tensor, $\underline{G}$ is a vector of the gravity forces, $\underline{T}$ is the vector of actuator efforts, and $\underline{\theta}$, $\dot{\underline{\theta}}$, and $\ddot{\underline{\theta}}$ are the 6 joint displacements, velocities and accelerations, respectively. The limits of the ith actuator may be any functions of θ_i and $\dot{\theta}_i$:

$$T_{imin}(\theta_i,\dot{\theta}_i) < T_i < T_{imax}(\theta_i,\dot{\theta}_i) \qquad (2)$$

The path of the end-effector is, $\underline{P} = \{x,y,z,w_1,w_2,w_3\}$, or $\{\underline{X},\underline{w}\}$, where $\underline{X}$, is the position of the path and $\underline{w}$ represents the orientation of the end effector fixed frame, H, with respect to inertial frame N (see Figure 1). Clearly $\underline{P}$ is a known function of the displacement along the path, S. The joint angles may be expressed in terms of the path variable S, using the kinematic transformation:

$$\underline{P}(S) = \underline{R}(\underline{\theta}) \qquad (3)$$

Differentiating Equation (3) twice with respect to time and solving for $\dot{\underline{\theta}}$ and $\ddot{\underline{\theta}}$ yields:

$$\dot{\underline{\theta}} = R_{\underline{\theta}}^{-1}\,\underline{P}_S\,\dot{S} \qquad (4)$$

$$\ddot{\underline{\theta}} = R_{\underline{\theta}}^{-1}\{\underline{P}_S\ddot{S} + \underline{P}_{SS}\dot{S}^2 - (R_{\underline{\theta}}^{-1}\underline{P}_S)^T R_{\underline{\theta}\underline{\theta}}(R_{\underline{\theta}}^{-1}\underline{P}_S)\dot{S}^2\}$$

where $R_{\underline{\theta}}$ is the Jacobian matrix, $R_{\underline{\theta}(i,j)} = \partial R_i / \partial\theta_j$. The partial derivatives of $R_{\underline{\theta}}$ with respect to $\underline{\theta}$ result in $R_{\underline{\theta}\underline{\theta}}$, the Hessian matrix. The s and $\underline{\theta}$ subscripts denote partial derivatives with respect to the scalar S and the vector $\underline{\theta}$ respectively.

The vectors $\underline{P}_S$ and $\underline{P}_{SS}$ can be written as $\{\underline{X}_S, \underline{w}_S\}$ and $\{\underline{X}_{SS}, \underline{w}_{SS}\}$. $\underline{X}_S$ is a unit vector tangent to the path, while $\underline{X}_{SS}$ is a vector of magnitude $1/\rho$ normal to the path, ρ being the radius of curvature of the path.

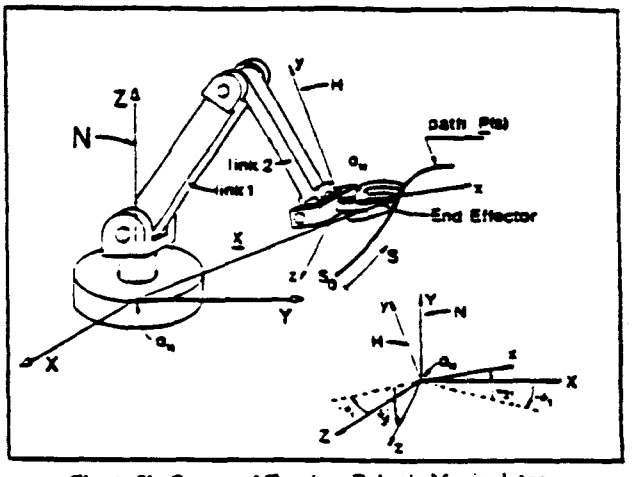

Fig. 1: Six Degree-of-Freedom Robotic Manipulator.

Substituting Equation (4) into Equation (1), yields the equation of motion in terms of $\underline{\theta}$, $\dot{S}$ and $\ddot{S}$:

$$\underline{m}(\underline{\theta})\,\ddot{S} + \underline{b}(\underline{\theta})\,\dot{S}^2 + \underline{G}(\underline{\theta}) = \underline{T} \qquad (5)$$

where $\underline{m}$ and $\underline{b}$ are defined in detail in Reference [4]. $\underline{\theta}$ can be obtained either explicitly or numerically as a function of S.

The objective of the optimization is to find the vector $\underline{T}$ that moves the manipulator along the path in minimum time. The transit time, J, may be written as:

$$J = \int_{S_0}^{S_f} \frac{dS}{\dot{S}} \qquad (6)$$

Reference [1] proves rigorously that J will be minimum if the acceleration along the path, $\ddot{S}$, is equal to either its maximum or the minimum permissible values, $\ddot{S}_+$ or $\ddot{S}_-$. Six values for $\ddot{S}$ are obtained by solving each row of Equation (5) for $\ddot{S}$:

$$\ddot{S}_i = \frac{T_i - b_i\,\dot{S}^2 - G_i}{m_i} \qquad (7)$$

The upper and lower bounds for each $\ddot{S}_i$ for given S and $\dot{S}$ are obtained by substituting the upper and lower bounds on $\underline{T}$ from Equation (2). The bars in Figure 2 represent the ranges of $\ddot{S}$ permitted by each actuator. Any acceleration out of the range of the ith actuator is beyond the capability of that actuator to keep the manipulator on its path. Clearly, the permissible

range of $\ddot{S}$ must lie in the common range of all the actuators. Thus:

$$\ddot{S}_d(S,\dot{S}) \le \ddot{S} \le \ddot{S}_a(S,\dot{S}) \qquad (8)$$

$$\ddot{S}_a = \min_i \left(\frac{T_{i\max} - b_i \dot{S}^2 - G_i}{m_i} \right)$$

$$\ddot{S}_d = \max_i \left(\frac{T_{i\min} - b_i \dot{S}^2 - G_i}{m_i} \right)$$

At each point, S, the bounds on $\ddot{S}$ are functions of the velocity $\dot{S}$. Generally, increasing $\dot{S}$ results in a decrease in the size of the permissible acceleration range. The velocity at which the permissible acceleration range is zero (or $\ddot{S}_a = \ddot{S}_d$) is the maximum permissible velocity, $\dot{S}_m$. For $\dot{S}$ greater than $\dot{S}_m$ no solution for the acceleration $\ddot{S}$ exists, which means that the manipulator is not capable of keeping its tip on the path. The values $\dot{S}_m$ as a function of S form the velocity limit curve, $\dot{S}_m(S)$, shown in Figure 3. At each point S, $\dot{S}_m$ is found by increasing $\dot{S}$ from zero until $\ddot{S}_a = \ddot{S}_d$.

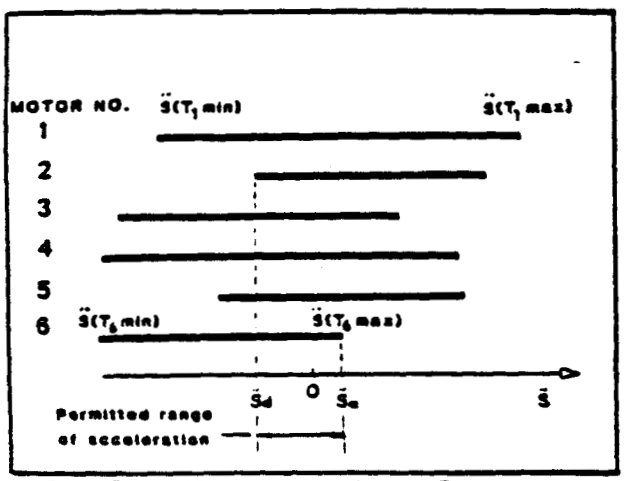

Fig. 2: Permissible Acceleration Along the Path for a Given Value of S and $\dot{S}$.

It might be noted that it is theoretically possible for the limit curve to form closed regions or be doubled valued[13], (see figure 3). This means that at these points on the path the actuators are too weak to keep the manipulator on the path at some low speed, but at a higher speed the manipulator could maintain its path by passing above those regions. However, operating in such a manner is not desirable and even potentially dangerous: If, while operating above a forbidden region the manipulator had to stop as quickly as possible on its path due to some problem, it would likely leave its path and could collide with an obstacle. Also our studies showed no such forbidden regions for systems with realistic parameters. Hence, OPTARM uses only the lowest value of $\dot{S}$, where $\ddot{S}_a = \ddot{S}_d$, to define the limit curve, as shown in Figure 3.

Reference [1] shows that the minimum time motion is achieved when $\ddot{S}$ is equal to either $\ddot{S}_a(S,\dot{S})$ or $\ddot{S}_d(S,\dot{S})$ at every point on the path. It also shows that the minimum time control problem is reduced to finding the switching points between $\ddot{S}_a(S,\dot{S})$ and $\ddot{S}_d(S,\dot{S})$ such that $\dot{S}$ is always maximum, but without having the trajectory in the phase plane cross the limit curve. Reference [1] presents the following algorithm, to find the optimal motion (refer to Figures 3):

1. Integrate $\ddot{S} = \ddot{S}_a(S,\dot{S})$ forward in time with the initial conditions S_0, and $\dot{S}_0$ until the trajectory intersects the $\dot{S}_m$ curve at some point a.

2. At point a, reduce the velocity along the dotted path until b, where if $\ddot{S} = \ddot{S}_d(S,\dot{S})$ is integrated forward until zero velocity, it coincides with $\dot{S}_m$ at some single point c, a point of tangency for continuous $\dot{S}_m$ curves.

3. From b, integrate $\ddot{S} = \ddot{S}_d(S,\dot{S})$ backward in time to yield the first switching point from acceleration to deceleration, d.

4. Point c is a switching point from deceleration to acceleration. From c, integrate $\ddot{S} = \ddot{S}_a(S,\dot{S})$ forward in time until either the final position, S_f, is reached, or the trajectory again intersects the $\dot{S}_m$ curve. If the $\dot{S}_m$ curve is intersected, repeat the process starting with step 2 at this intersection point. Note that at point c the maximum acceleration and the maximum deceleration are the same.

5. From S_f and $\dot{S}_f$, integrate $\ddot{S} = \ddot{S}_d(S,\dot{S})$ backward in time to find the final switching point at e.

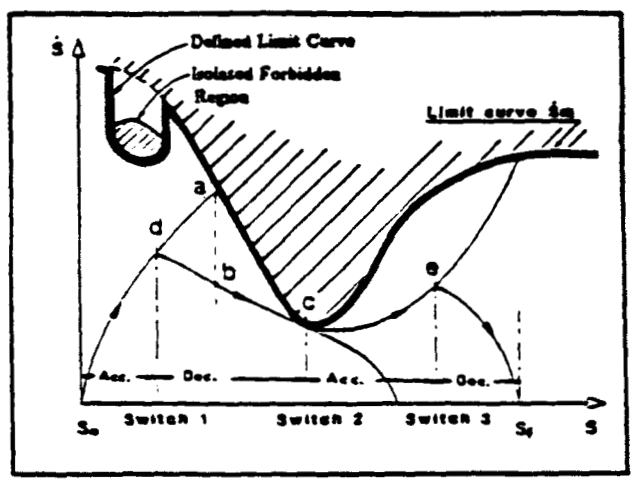

Fig. 3: Construction of the Optimal Trajectory in the Phase Plane.

Once the optimal trajectory is obtained, the optimal values of $\dot{\theta}$, $\ddot{\theta}$ and $T(\theta)$ are computed, using Equations (3) to (5). Note that the initial and final velocities do not need to be zero.

This technique may be extended to include other constraints that can be expressed as functions of S, $\dot{S}$ and $\ddot{S}$, in addition to those on the actuators. These constraints are transformed into bounds on $\ddot{S}(S,\dot{S})$ and form additional bars in Figure 2. OPTARM contains constraints on the payload acceleration and the gripping force which

satisfy the above condition. Simple examples of this procedure are presented below. First, the limits on the payload dynamic force is considered with the form:

$$|\ddot{\underline{X}}| \leq a_m \tag{9}$$

where a_m is the maximum allowable inertial acceleration of the payload, $\ddot{\underline{X}}$. If the path, position $\underline{X}$, shown in Figure 1, is defined by the position of the payload center of mass, then $\ddot{\underline{X}}$ is given by:

$$\ddot{\underline{X}} = \underline{X}_{ss}\dot{S}^2 + \underline{X}_s\ddot{S} \tag{10}$$

where $\underline{X}_s$ and $\underline{X}_{ss}$ are the first three elments of $\underline{P}_s$ and $\underline{P}_{ss}$ in Equation (4) respectively. Substituting Equation (10) into Equation (9) and solving for $\ddot{S}$ yields:

$$\begin{aligned} \ddot{S}_u &\leq \sqrt{a_m^2 - \underline{X}_{ss}^2\dot{S}^4} \\ \ddot{S}_d &\geq -\sqrt{a_m^2 - \underline{X}_{ss}^2\dot{S}^4} \end{aligned} \tag{11}$$

Equation set (11) bounds the acceleration $\ddot{S}$ as a function of a_m and the velocity $\dot{S}$; this limit is added to those of the actuators in forming Equation set (8).

Second, the following simple example shows how to obtain the constraints imposed by the gripping force. For the simple parallel jaw gripper, shown in Figure 4, the payload inertial force acting parallel to gripper surface must not exceed the friction forces between the payload and the gripper jaws, if the object is not to be pulled from the gripper. Gravity is neglected for the sake of clarity. First the inertial acceleration $\ddot{\underline{X}}$ of the center of mass of the payload is resolved into two perpendicular components, $\ddot{\underline{X}}_a$ and $\ddot{\underline{X}}_t$, shown in Figure 4. $\ddot{\underline{X}}_a$ is the component in the z direction, and $\ddot{\underline{X}}_t$ is the component in the x-y plane. The magnitudes of $\ddot{\underline{X}}_a$ and $\ddot{\underline{X}}_t$ are given by:

$$\ddot{X}_a = \ddot{\underline{X}} \cdot \underline{e}_z \tag{12}$$

$$\ddot{X}_t = \sqrt{\ddot{X}^2 - \ddot{X}_a^2} \tag{13}$$

where $\underline{e}_z$ is the unit vector in the z direction of the gripper frame. The friction forces act parallel to the x-y plane. The total friction force, F_f is limited by:

$$F_f \leq 2\mu F_g + \mu m_p |\ddot{X}_a| \tag{14}$$

where m_p is the mass of the payload, μ is the coefficient of friction between the payload and the gripper surfaces, and F_g is the applied squeeze force. The presentation does not consider rotations within the gripper, although these can be included in a similar manner. To maintain a firm grip the component of the inertial force acting on the payload in the x-y plane is limited by the maximum F_f:

$$m_p \ddot{X}_t \leq 2\mu F_g + \mu m_p |\ddot{X}_a| \tag{15}$$

Substituting Equations (10), (12) and (13) into Equation (15) yields the following quadratic equation in $\ddot{S}$:

$$a\ddot{S}^2 + b\ddot{S} + c \leq 0 \tag{16}$$

where

$$a = m_p^2\{1 - (1+\mu^2)v^2\} \tag{17}$$

$$b = -2m_p^2 u \cdot v(1+\mu^2)\dot{S}^2 - 4\mu^2 m_p F_g v \cdot \mathrm{sign}(u\dot{S}^2 + v\ddot{S})$$

$$c = m_p^2\{\underline{X}_{ss}^2 - (1+\mu^2)u^2\}\dot{S}^4 - 4\mu^2 m_p F_g u \cdot \mathrm{sign}(u\dot{S}^2 + v\ddot{S})\dot{S}^2 - (2\mu F_g)^2$$

and

$$v = \underline{X}_s \cdot \underline{e}_z$$

$$u = \underline{X}_{ss} \cdot \underline{e}_z$$

The solutions to Equation (16) define the bounds on $\ddot{S}$ due to the constraint on the gripping force. These bounds depend on the path through $\underline{X}_s$ and $\underline{X}_{ss}$, the orientation of the gripper through $\underline{e}_z$, the applied squeezing force, F_g, the payload mass, m_p, and the coefficient of friction, μ. The existance of a solution for $\ddot{S}$ in Equation (16) depends on the value of the velocity $\dot{S}$. The lowest positive value of $\dot{S}$ for which no solution exists defines the velocity limit $\dot{S}_m$. The bounds on the acceleration in Equation (16) are applied in OPTARM in a similar manner as the other constraints discussed earlier.

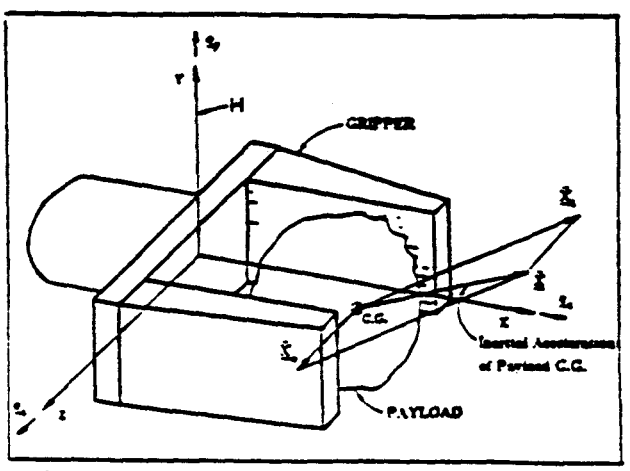

Fig. 4: The Absolute Acceleration of Payload C.G. and its Components in the Gripper Fixed Frame.

III. OPTARM

This algorithm has been implemented in a program called OPTARM for six degree-of-freedom manipulators. It considers the three dimensional paths and end-effector motions with straight lines, circular curves and splines. It computes the full nonlinear dynamic matrices of the manipulator and the path characteristics at, typically several hundred, discrete points along the path. Other OPTARM's outputs are the actuator torques for the dynamic feed-forward control, the joint positions, velocities and accelerations for closed loop control, and includes other important information for the designer like the actuators' power. OPTARM, is written in FORTRAN and requires less than 30 seconds of computation time on a mini-computer PDP 11/44 to complete a full

optimization of a typical industrial manipulator, including the graphics computations. The relatively short computation times and its interactive graphics make the program an effective tool for improving manipulator dynamic performance, manipulator design, and the design of their tasks and work places, as demonstrated in the following examples.

IV. Examples

The following examples are presented to demonstrate capabilities of the OPTARM program using the six degree-of-freedom manipulator, shown in Figure 1. The parameters of this manipulator are given in Table 1.

Table 1: Manipulator Parameters.

	L meter	L_{cg} meter	Mass Kg	Principal Moment of Inertia about C.G., Kgm^2		
Link 1:	1.0	0.3	7.0	0.0	1.0	1.0
Link 2:	1.0	0.3	5.0	0.0	1.0	1.0
Link 3:	0.25	0.25	3.0	0.0	0.25	0.25

The first example shows the typical improvement in performance over conventional control which can be obtained by using OPTARM. All the figures shown are hard copies of OPTARM graphic displays. Figure 5 shows a three dimensional view of the manipulator moving from rest at point A, (0,0,1.5), along a straight line directed toward point (1.7,0.5,0). At point B it takes a circular curve of 0.5 m radius to point C, then goes finally along a straight line to point D, (1.3,0.5,-1.3). During the move the end-effector remains parallel to the X axis. Figure 6 shows the phase plane trajectory of the optimal motion for this path. Note that the maximum acceleration can be negative in some range of the trajectory. The time required for the motion is 1.185 seconds. The use of conventional control with constant acceleration velocity and deceleration, also shown in Figure 6, required 1.675 seconds, 41% longer. This substantial improvement in the traveling time required no change in the manipulator's hardware. Moreover, by using OPTARM interactively, it was shown that the traveling time could be reduced further by an additional 21% to 0.930 seconds while still moving between the same end points by increasing the radius of the curved section of the path from 0.5 to 1.5 meters. This shows the potential of the technique to select a better path for a given task.

The next example shows an improvement in system performance by an OPTARM modification of system design. Figure 7 shows an optimal trajectory along a path with a similar form as in the first example, except that it starts at (0.25,0,1.3), towards point (1.3,0.5,1.3), and stops at point (1.3,0.5,-1.3); the curve radius is 1 meter. The optimal motion for this path is 1.076 sec., and has only one switching point. As can be seen in Figure 7 the trajectory does not approach the limit curve, suggesting that the system is over-designed for this task. The first three actuator torques are shown in Figure 8. OPTARM provides all 6 actuator torques. At each point on the path, one of the 6 actuators is at its limit. It can be seen that actuator 3 is never near its limit. Reducing its size reduces the motion time because its reduced weight lowers the load on the other actuators. Figure 9 shows the optimal trajectory along the same path with actuator 3 torque level and weight reduced by 50%. The time decreased from 1.076 seconds to 1.043 seconds. Even though the reduction in time is not large in this case it does demonstrate that properly selected smaller actuators can increase manipulator quickness in some cases.

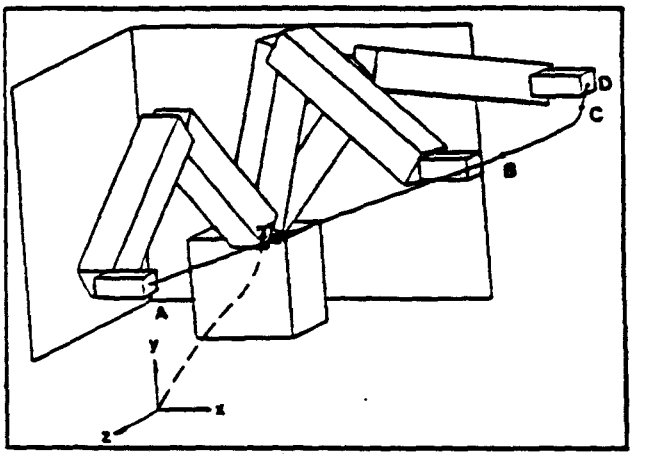

Fig. 5: Manipulator's configuration at selected points along Path #1.

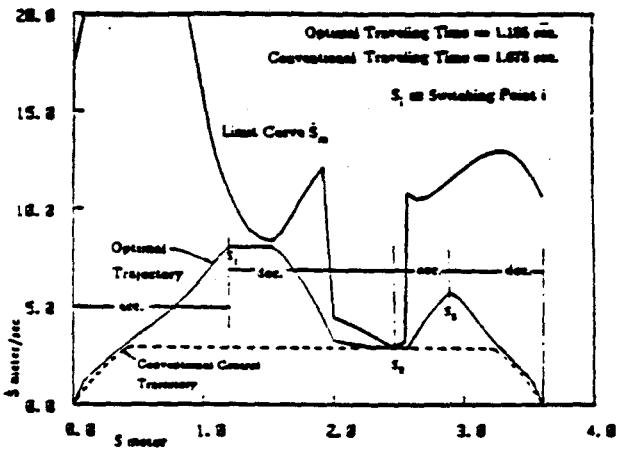

Fig. 6: Phase Plane Plots for Path #1, for Conventional and Optimal Controllers.

The next example shows the performance improvement resulting from a redesign of the work place. First the manipulator moves from one work-station to the next along a straight line from point (0,0,1.3) to (1.0,0.5,-1.3). Note that the initial and final velocities are not zero at these points, as might be required if these work-stations were moving conveyer belts. The traveling time of the optimal trajectory was 1.050 sec.. A move of the two end-points away from the base of the manipulator by (0.5,0,0), resulted in the optimal trajectory shown in Figure 10 and a

reduction in time by 49% to 0.530 seconds. The case also demonstrates that the initial or final velocities need not be zero.

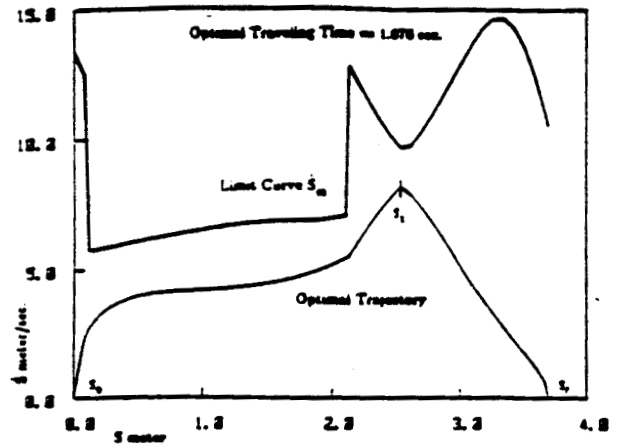

Fig. 7: Optimal Trajectory for Path #2 with Oversized Actuator 3.

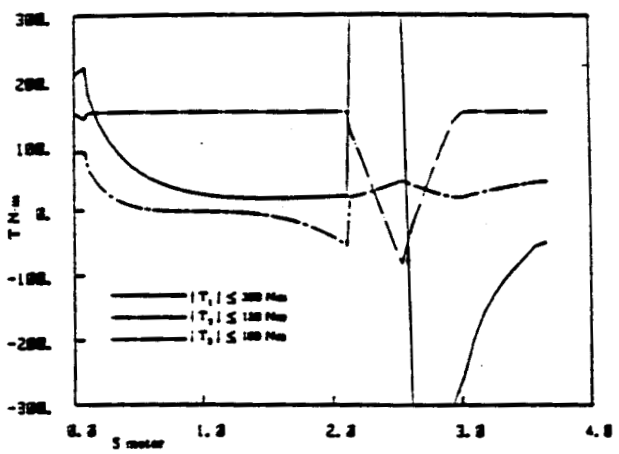

Fig. 8: Joint Actuator Torques as a Function of S.

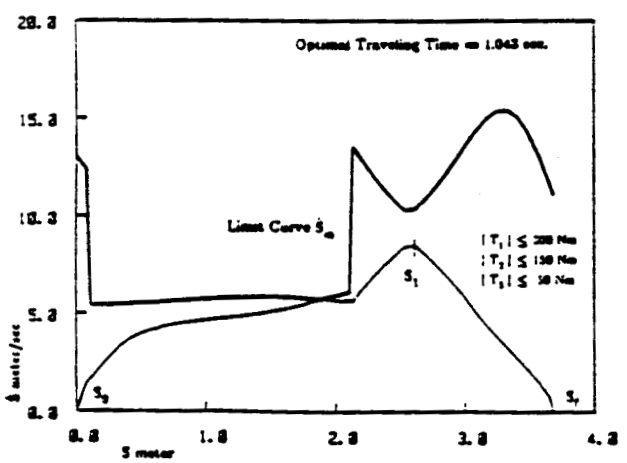

Fig. 9: Optimal Trajectory for Path #2 with Reduced Actuator 3.

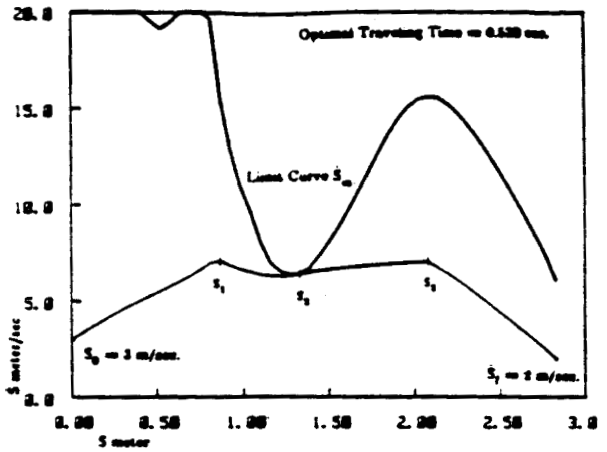

Fig. 10: Optimal Trajectory Along a Straight Line with Nonzero Initial and Final Velocities.

Figure 11 shows the effect of constraints on payload acceleration on the optimal trajectory. The optimal trajectory, using the same path as in the first example, path #1, with a constraint on the payload acceleration of 20 m/sec.^{2} (2 g's) results in a constant velocity along the circular curve; the centrifugal dynamic force (with the payload mass being 1 Kg) was equal to the limit on the acceleration.

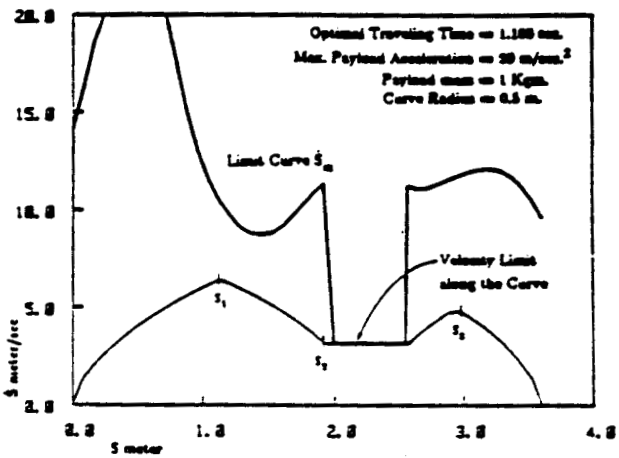

Fig. 11: Optimal Trajectory for Path # 1 with a Limit on the Payload Acceleration.

V. Conclusions

This paper shows that a recently developed algorithm is practical for the time optimal control of six degree-of-freedom manipulators moving along a prescribed path subject to actuator constraints. Such optimal motion is shown to be significantly faster than conventional control strategies currently in use and can lead to greater system productivity. The algorithm is extended to include constraints on the gripping force and on the payload acceleration. It also describes an interactive CAD implementation of the algorithm, OPTARM, and examples are presented of its use to optimize manipulator performance, designs, tasks and work places.

VI. Acknowledgements

The authors would like to acknowledge the support of this research by the National Aeronautics and Space Administration, Langley Research Center, Hampton, VA under grant NAG-1-439, Supplement No. 1.

VII. References

1. Bobrow J.E., " Optimal control of manipulators", Ph.D. Thesis 1982, University of California Los Angeles.

2. Bobrow, J.E., Dubowsky, S., and Gibson, J.S., "On the Optimal Control of Robotic Manipulators with Actuators Constraints, "Proc. of the 1983 American Control Conf. San Francisco, CA, pp. 782-787, June 1983.

3. Dubowsky, S., Shiller, Z., "Optimal Dynamic Trajectories for Robotic Manipulators, "Proceedings of the V CISM-IFToMM Symposium on the Theory and Practice of Robots and Manipulators, June 1984, Udine, Italy.

4. Shiller, Z. "Optimal Dynamic Trajectories and Modeling of Robotic Manipulators", M.Sc. Thesis, Massachusetts Institute of Technology, June 1984.

5. Blubaugh, T. "Time-Optimal Planning of Point to Point Moves for Robotic Manipulators", M.Sc. Thesis, Massachusetts Institute of Technology, December 1984.

6. Kahn M.E., and Roth B., "The Near-Minimum-Time Control of Open-Loop Articulated Kinematic Chains". Journal of Dynamic Systems, Measurment and Control, vol. 93, No. 3, Sept. 1971, pp. 164-172.

7. Scheinman, V., and Roth, B. "On the Optimal Selection and Placement of Manipulators", Proceedings of the V CISM-IFToMM Symposium on the Theory and Practice of Robots and Manipulators, June 1984, Udine, Italy.

8. Kiriazov, P., and Marinov, P. "A Method for Time-Optimal Control of Dynamically Constrained Manipulators", Proceedings of the V CISM-IFToMM Symposium on the Theory and Practice of Robots and Manipulators, June 1984, Udine, Italy.

9. Luh, J.Y.S., and Lin, C.S., "Optimum Path Planning for Mechanical Manipulators, "Journal of Dynamic Systems, Measurment, and Control, Vol. 102, No. 2, June 1981, pp. 142-151.

10. Luh, J.Y.S., and Walker, M.W., "Minimum-Time Along the Path for a Mechanical Arm, "Proc. of the IEEE Conference on Decision and Control, December 1977, New Orleans, LA, pp. 755-759.

11. Hollerbach, J.M. "Dynamic Scaling of Manipulator Trajectories", J. Dynamic Systems, Measurment, and Control, Vol. 106, pp. 102-106, March 1984.

12. Sahar, G. "Planning of Minimum-Time Trajectories for Robot Arms", Ocean Engineer Thesis, Department of Ocean Engineering, Massachusetts Institute of Technology, September 1984.

13. Shin, K.G. and McKay, N.D. "An Efficient Robot Arm Control Under Geometric Path Constraints",Proc. 22nd IEEE Conf. Decision and Control, 1499-1457, San Antonio, Texas, 1983.

APPENDIX III

TIME OPTIMAL TRAJECTORY PLANNING FOR ROBOTIC MANIPULATORS WITH OBSTACLE AVOIDANCE: A CAD APPROACH